Il presente lavoro è stato pubblicato su Applied Clay Science 152 (2018) 9–21con doi https://doi.org/10.1016/j.clay.2017.11.036

Effects of processing on the mineralogy and solubility of carbonate-rich clays for alkaline activation purpose: mechanical, thermal activation in red/ox atmosphere and their combination

A. D'Elia[a, *], D. Pinto[a], G. Eramo[a], L.C. Giannossa[b], G. Ventruti[a], R. Laviano[a]

[a] *Dipartimento di Scienze della Terra e Geoambientali, Università degli Studi di Bari "Aldo Moro", Bari, Italy*
[b] *Dipartimento di Chimica, Università degli Studi di Bari "Aldo Moro", Bari, Italy*

Corresponding author. angela.delia@uniba.it

Abstract. The present study focuses on the assessment of the effects of different activation methods on carbonate-rich clays, to understand the mineralogical differences originated and to exploit such information to industry for traditional and innovative applications, especially as a precursor for alkali activated binders.
Illite carbonate-rich clay samples were subjected to thermal activation in ox/red atmosphere between 400 and 900 °C, mechanical activation (grinding for 5, 10 and 15 min) and to a combination of such treatments. Mineralogical and textural changes in the activated samples were evaluated through X-ray powder diffraction, Fourier transform infrared spectroscopy and thermal techniques. The activated samples with the highest content of amorphous phase underwent leaching tests in a 3 M NaOH solution by means of inductively coupled plasma-mass spectrometry. The application of the three processing rou- tines, yielded three types of activated clays with different leaching modes of Si, Al, K and Ca: (1) high energy grinding preferentially delaminates clay minerals and reduces the grain size of calcite. K leaching reaches the highest values; (2) thermal heating at 800 °C increases relatively the Si/Al solubility ratio, but the absolute con- centrations of these elements are equal or lower than those obtained from ground clays. The relatively higher leaching of Ca is influenced by the formation of non-stoichiometric and poorly crystalline Ca-silicates and -alu- minosilicates; (3) high energy grinding combined with heating treatment yields an extended amorphisation, mainly at the expense of clay minerals, with the highest leaching of Si and Al, and the lowest of Ca. New formed K-feldspars inhibit the concentration of K in alkaline solution

Keywords: Thermal activation Mechanical activation Illite clays Carbonates

1. Introduction

Natural clays are important industrial raw materials used directly or in combination with other materials for the production of structural ceramics and building materials. In the recent years, there has been increasing interest in studying the use of such natural feedstocks for the synthesis of alkali-activated binders, because of their low cost and abundance in most countries. The literature on the subject remains scarce and further efforts could be made to better understand the potential of such complex systems.

Alkali-activated materials are inorganic binders obtained by alkaline or alkaline-earth activation of aluminosilicates and represent nowadays a greener alternative to ordinary Portland cement, owing to their low-CO_2 emission for their production at relatively mild temperature (below 100 °C) and their good thermal (Cheng and Chiu 2003; Kamseu et al. 2010), chemical (Bakharev 2005; Palomo et al. 1999a) and mechanical (Lee and van Deventer 2002) properties.

A large number of studies have focused on the synthesis of these novel engineering materials from calcined kaolinitic clays (metakaolinite) (e.g. Barbosa et al. 2000; Davidovits, 1991; De Silva et al. 2007; Duxson et al., 2007a, b; Granizo et al. 2000; Palomo et al. 1999a), or from fly ash, blast furnace slag and other industrial by-products too (Buchwald 2006; Duxson et al. 2007a; Palomo et al. 1999b; van Jaarsveld et al. 2002). Recently, the suitability of common clays other than kaolinite for geopolymeric purpose have been also investigated as they represent widely available and relatively cheap raw materi- als and may show a certain reactivity after the activation processing

(Buchwald et al. 2009; Ferone et al. 2013, 2015; Ruiz-Santaquiteria et al. 2013; Seiffarth et al., 2013). The reactivity of clays can be in fact increased by using an appropriate activation treatment, i.e. thermal (He et al. 1995a) or mechanical (MacKenzie et al. 2007a). The thermal treatment, which is the most used activation strategy, transforms clays in a disordered metastable state (Fernandez et al. 2011; He et al. 1994, 1995a, 1995b; Tironi et al. 2013) by effect of the dehydroxylation of clay minerals occurring in the temperature range between 500 and 800 °C, which enhances the solubility in alkaline solution of the derived amorphous to low crystalline phases (Buchwald et al. 2009; Essaidi et al. 2013, 2014, Ferone et al. 2013, 2015; Kaps and Hohmann 2010; Ruiz-Santaquiteria et al. 2013; Seiffarth et al., 2013). The reaction mechanisms concerning the thermal activation of natural clay resources are affected by the complex nature of these materials, as well as by the specific operating conditions of the heating treatment (Habert et al. 2009; Snellings et al. 2012). In particular, the presence of secondary minerals and contaminants other than silicoaluminates in the raw materials can affect the properties of the final products and add reaction pathways during alkali activation (Mackenzie and Welter 2014).

The adoption of a mild reducing atmosphere during thermal treatments can represent a more ecological method, although poorly studied, to enhance the clay reactivity at lower temperatures compared to the commonly adopted oxidising regime (Seiffarth et al., 2013). In the case of carbonate-rich clays the reducing regime can also increase the temperature range which separates the achievement of the maximum clay reactivity and the occurrence of crystalline high-temperature phases (Bauluz et al. 2003; Carretero et al. 2002; Cultrone et al. 2001; Duminuco et al. 1998; Gonzalez Garcia et al. 1991; Letsch and Noll 1983; Maggetti et al. 2011; Maritan et al. 2006; Rathossi and Pontikes 2010; Riccardi et al. 1999; Tschegg et al., 2009), less reactive with respect to the alkali activation.

The mechanochemical activation, performed through high energy grinding, can represent another sustainable and time saving alternative to amorphise clays compared to the calcination process, but currently is scarcely considered as activation procedure of clays for the production of alkaline binders (Mackenzie et al., 2007). Several studies demonstrated that the mechanochemical activation can be used to obtain an amorphous material by breaking the clay bonds and the original OH groups to form new particles aggregates of increased porosity, specific surface area, altered cation-exchange capacity and solubility (Baláž 2003; Balek et al. 2007; Gonzalez Garcia et al. 1991; Hamzaoui et al. 2015; MacKenzie et al. 2007; Suraj et al. 1997; Sánchez-Soto and Pérez-Rodriguez, 1989; Sánchez-Soto et al., 1994, 2000).

Grinding also influences the thermal behaviour of clay minerals, enhancing phase transformations during heating (Balek et al. 2007; Sánchez-Soto and Pérez-Rodriguez, 1989; Sánchez-Soto et al., 1994) and can represent a valid method to enhance the reactivity at lower temperatures of heated clays, interested by previous changes in their physico-chemical properties. However, there is a lack of literature dealing with the mechanical activation of three-layer clay minerals as geopolymeric raw materials and in particular, the application of both mechanical and thermal treatments promoting clay activation for the geopolymer production represents a never investigated field.

Despite the literature on inexpensive clays to synthesize novel activated materials is rapidly growing, the use of illite carbonate-rich clays has been scarcely explored (Ferone et al. 2013, 2015) although it may have some advantages (Ferone et al. 2015; Yip et al. 2005, 2008). In particular, it has been proven that the Ca addition, as lime and calcium hydroxide, contributes positively to improve the compressive strength of the resulting geopolymeric products, owing to the formation of a C-S-H/C-A-S-H gel (Temuujin et al. 2009; Khater 2012) which may enhance the precipitation of dissolved monomers acting as nucleation centers (Khater 2012; Temuujin et al. 2009) and may increase the alkalinity of the system, favouring the co-precipitation of the geopolymeric N-A-S-H gel and giving place to an homogeneous and strong structure (Khater 2012). Geopolymerisation is favoured by the formation of the C-S-H gel whose growth is controlled not only by activation parameters (alkalinity of the activator, curing temperature, etc.) (Khater 2012) but also by the nature, crystallinity and particle size of the added Ca-bearing sources (Yip et al. 2008).

Owing to the chemical and mineralogical complexity of such a clay mixture, several factors are expected to concur and enhance their reactivity for the geopolymeric purpose and, in this connection, the choice of the activation strategy may represent a key point. Different activation methods are expected to exert different effects both on the degree of clay mineral decomposition and on the crystallinity of carbonates, influencing their solubility in the alkaline medium as well as the possibility for calcium compounds to participate to the geopolymerisation as charge balancing cations or to act as fillers (García-Lodeiro et al. 2010, 2011, 2012, 2013; Khater 2012; Yip et al. 2005, 2008).

In this perspective, the present study is focused on the assessment of the effects of different activation strategies on the reactivity of carbonate-rich clays, to gain a deeper insight in the phase transformations occurring in the samples after each treatment and to exploit such information for technological transferability to industry. With this aim, illite carbonate-rich clays from the Apulian region (southern Italy) were subjected to different activation treatments in order to explore their effectiveness in promoting the loss of crystallinity (and thus reactivity) of the clay minerals and at the same time to produce the highest availability of calcium from calcium-bearing minerals. Besides the more explored thermal activation processing, a mechanical activation by vibratory milling, which represents a more ecological pre-treatment methodology, has been used for the first time in this study for the activation of illite carbonate-rich clays, in addition to the combination of both mechanical and thermal treatments, which represents an energy-saving processing favouring clay mineral dehydroxylation reactions. The use of both oxidising and mild reducing conditions during thermal treatments was also tested, in order to evaluate potentially positive effects of the adoption of different burning regimes on clay mineral decomposition reactions. Results of different activation strategies were carefully investigated by using a multianalytical approach and the potential suitability of the resulting treated clays as raw materials for the production of alkali-activated binders was evaluated and discussed on the basis of results of solubility test in a NaOH solution.

2. Experimental

The raw materials involved in the present study are Apulian calcareous-rich clay sediments belonging to "Argille subappennine" formation. The sample, labelled as "LCR", was collected from a clay deposit (Lucera, FG) exploited for structural ceramics.

To increase its reactivity, the investigated clay was subjected to different treatments: mechanical, thermal, combination of mechanical and thermal treatments (Fig. 1). For the mechanical treatment, clay portions of 4 g each were prepared after quartering the whole sample and oven drying at temperature of 50 ± 5 °C. Selected samples were dry ground in a vibratory ball mill for 5, 10, and 15 min at a frequency of 30 Hz (1800 min^{-1}) using a Retsch MM 400 instrument equipped with two 25 ml tungsten carbide grinding jars with screwable cover and each fitted with 2 tungsten carbide balls of 1.5 mm in diameter. Grinding conditions were evaluated taking into account information from literature (MacKenzie et al., 2007) and on the basis of several preliminary tests. Accordingly, a 5 min milling time (at 30 Hz) resulted to be the minimum time interval for the achievement of an extensive crystallinity loss of clay minerals (detectable by X-ray diffraction); doubling and tripling this time has been chosen in order to verify the effects of the prolongation of grinding on the amorphisation process. Larger times were not considered because they showed significant particle ag-

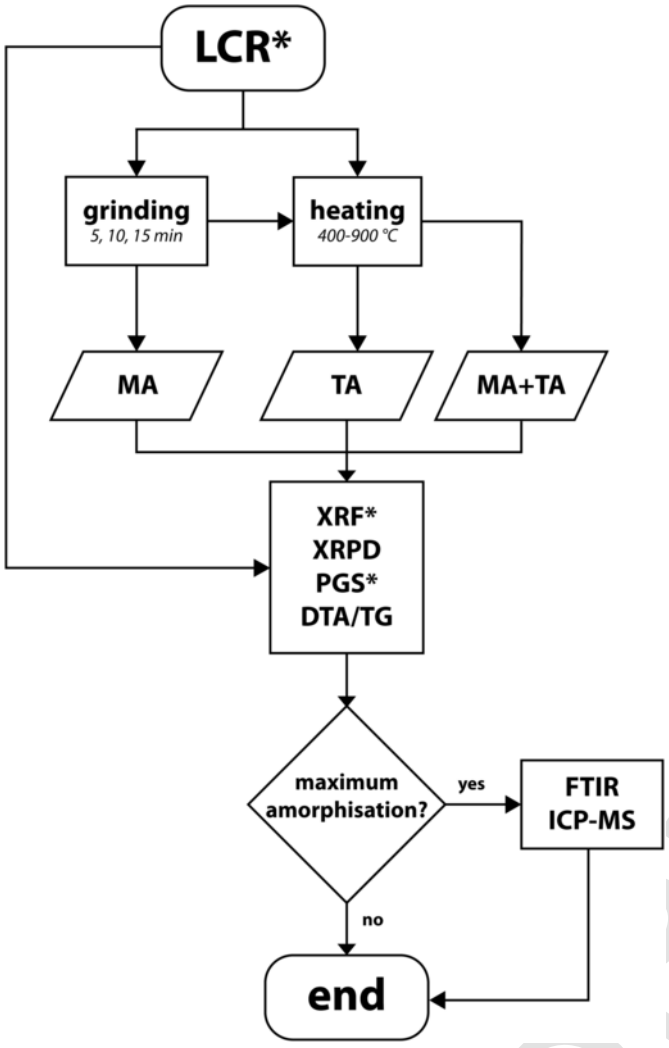

Fig. 1. Activation procedures on LCR clay. MA = mechanical activation, TA = thermal activation.

gregation effects. The thermal treatment was carried out by heating clay samples in a laboratory muffle furnace after placing them in crucibles. A gentle milling in vibratory mill at a frequency of 10 Hz for 120 s was performed to ensure sample homogenisation before heating. Samples were then thermally treated for 1 h at the temperatures of 400, 500, 600, 700, 800 and 900 °C under both oxidising and almost reducing burning conditions, with an average heating rate of about 13 °C/min, and cooled in the oven to room temperature. The almost reducing at- mosphere was achieved providing the crucibles by lids, thus heating the samples in the degassing atmosphere of the clays, according to a proce- dure followed in literature (Seiffarth et al., 2013). To evaluate the ef- fects of the combination of the two kinds of treatments on clays reactiv- ity, clay samples were subjected to mechanical pre-treatments and suc- cessively to thermal treatments, by using the same conditions described above for each treatment alone. In order to verify the reproducibility of each activation method, three replicas of all mechanical, thermal treatments both in oxidising and reducing conditions, and combinations of mechanical and thermal treatments have been carried out. To this purpose, a total of 108 clay portions were selected.

Major oxides and trace element concentrations of raw clay were determined on pressed powder pellets by an automatic spectrometer Panalytical AXIOS-Advanced, equipped with an X-ray tube X SST-mAX (Rh anode), following literature data (Franzini et al. 1972, 1975) to cor- rect the matrix effects. The detection limit for major element oxides was 0.01 wt%. Two reference standards (AGV-1 from USGS - USA and NIM-G from NIM - South Africa) were used to check the accuracy of the analytical data. Volatile components (H_2O plus CO_2) were measured with the loss on ignition (LOI).

The particle size distribution of the raw clay in the fraction between 2 mm and 32 μm was obtained by wet sieving, while sedimentation, according to Stoke's law, was applied for particles size < 32 μm (Tickell 1965).

The mineralogical characterization of the untreated clay samples and activated clays was determined by X-ray powder diffraction (XRPD) using a PANalytical Empyrean diffractometer equipped with a Real Time Multiple Strip (RTMS) *PIXcel*^{3D} detector and Cu-Kα radiation. Analytical conditions were: 40 mA and 40 kV, 2θ range from 3 to 80°, virtual scan of 0.026°2θ, counting time 360 s per step. The incident beam pathway included a 0.125° divergence slit, a 0.25° antiscattering slit and a soller slit (0.02 rad), whereas a Ni filter, a soller slit (0.02 rad) and an antiscatter blade (7.5 mm) were mounted in the diffracted pathway. For preliminary identification of clay minerals in the raw material, XRPD analyses were performed on oriented air-dried specimens (fraction <2 μm), glycolated at 60 °C for 8 h and heated at 550 °C. Percentage of illite (%I) and stacking order (Reichweite; R) of the I-Sm mixed layer were determined on X-ray patterns of glycolated oriented specimens according to Moore and Reynolds (1997). Qualitative and quantitative mineralogical analyses were carried out on bulk samples side-loaded in plexiglass sample holders. To ensure the best particle statistics for X-ray diffraction with minimum damage on the samples, ground powders were obtained with the Retsch MM 400 vibratory mill using the following conditions: wet milling in ethanol at the frequency of 20 Hz for 120 s in the case of the untreated clay and dry milling for 60 s at the frequency of 10 Hz in the case of the activated clay samples. X-ray patterns were analysed using the software X'Pert High Score 3.0e which includes ICSD database, whereas phase quantification was carried out by means of the Rietveld refinement software BGMN (Bergmann et al. 1998) using the new graphical user interface *Profex* (Doebelin and Kleeberg 2015). Rietveld refinements were performed by using modified structure models contained in the BGMN database and from Ufer et al. (2012a, 2012b) in the case of I-Sm interstratifications. In order to quantify the amorphous phase in the clay after thermal and mechanical treatments, the Rietveld technique was combined with the internal standard method by adding corundum (10 wt%) to the samples (Gualtieri 2000).

Differential thermal and thermogravimetric analysis (DTA/TG/DTG) were performed by means of a Toshiba STA7200RV analyser, on about 20 mg of each sample placed in alumina crucibles. Samples were examined over the range from 30 to 900 °C using a heating rate of 10 °C/min in a nitrogen flow (60 ml/min).

Fourier transform infrared (FTIR) measurements were acquired using a Nicolet 380 FTIR spectrometer equipped with an EverGlo source, a KBr beamsplitter and a deuterated triglycine sulfate (DTGS) detector. FTIR spectra were collected in transmission mode on pellets of 13 mm discs with approximately 2 mg of the same sample powders used for XRPD, which were diluted in 200 mg of KBr to record optimal spectra in the regions of 4000-400 cm^{-1}. The pellets were also dried at 110 °C for at least 12 h to minimise possible adsorbed water. The nominal resolution was set to 4 cm^{-1}; 128 scans over the range 400-4000 cm^{-1} were averaged for each sample and background. The identification of phases was based on the comparison of the results of our study with the corresponding literature data.

The amount of reactive species of untreated and treated samples were determined after leaching test in basic medium by mixing 0.5000 ± 0.0005 g of each sample with 20 ml of a 3 M NaOH solution (Ferone et al. 2015; Xu and van Deventer, 2002). After stirring for 5 h at room temperature, the solutions and solid residues were separated

by filtering using a Büchner funnel provided by 0.45 μm PTFE mem- brane filters. The concentration of the NaOH solution was chosen by a comparison with literature tests on similar clay sources subjected to thermal treatments (Ferone et al. 2015). Moreover, the selected alka- linity of the solution is similar to that required for the alkali activation of aluminosilicates with high calcium content (e.g. blast furnace slag, Fernández-Jiménez et al. 1999; Fernández-Jiménez and Puertas, 2001). To achieve a pH value of the solutions suitable for the ICP-MS analysis, 1 ml of each sample solution has been diluted with 2% HNO_3 up to a 100 ml final volume. Al, Ca, Si and K elemental analyses of the filtered solutions were determined by an inductively coupled plasma-mass spec- trometer (NexION 300X PerkinElmer ICP-MS spectrometer) equipped with a collision cell. External calibration with matrix matching stan- dards was employed for quantification. All experimental data were av- eraged on three replicates.

3. Results

3.1. Chemical and grain size analysis

The clay sediment used as raw material in this study consists mainly of the particle fraction smaller than 63 μm, which represents about 90.40% of the total dry mass of the sample and is composed of 42.86% clay (< 4 μm) and 47.54% silt (Fig. 2). According to Shepard's classifi- cation (1954) the sample falls into the "clayey silt" field.

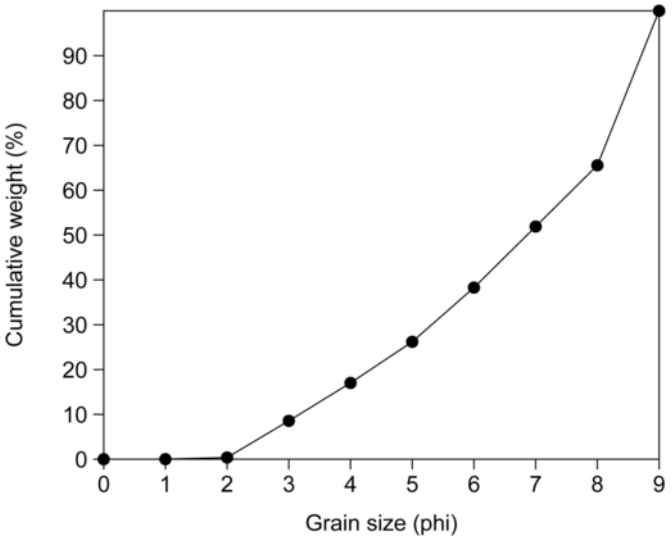

Fig. 2. Grain size distribution of LCR clay.

Chemical analyses by XRF showed that SiO_2, Al_2O_3 and CaO are the main components of the sediment, whereas Fe_2O_3, MgO and K_2O are present in lower concentrations. Only small percentages of other oxides such as MnO, Na_2O and TiO_2 are observed (Table 1). A loss on ignition value (LOI) of 20.32 wt% was measured from mass variations of the clay due to the loss of volatile components from hydrated silicates and car- bonates after heating at 950 °C.

3.2. XRPD

The X-ray pattern of the unprocessed clay shows clearly visible first order reflections of illite/muscovite, two almost overlapped reflec- tions at about 12.5°2θ corresponding to kaolinite and chlorite and a broad shaped band at around 5°2θ attributed to a disordered (Reich- weite R0) smectite-rich I-Sm intestratification with 30% illitic layers (R0 I(0.3)-Sm) on the basis of X-ray diffraction measurements on glycolated oriented samples (Moore and Reynolds, 1997).

According to QPA by Rietveld refinement (Fig. 3) about 35 wt% of the sediment consists of clay minerals in well agreement with grain size analyses, 32 wt% of carbonates (mainly calcite), 17 wt% of quartz, while minor amounts of feldspars and iron hydroxides are also present (Table 1). The good match between the bulk chemical composition re- calculated from mineralogical data and XRF chemical data (Table 1) gives an estimation of the accuracy of the Rietveld results. The only ex- ception is represented by the value of Fe_2O_3 oxide, due to the occurrence of low crystalline Fe-oxides and hydroxides not detectable by X-ray dif- fraction, but accounted by the slight amorphous phase content of the clay. The loss on ignition value, mainly related to the abundance of hy- drated silicates and carbonates, is also very close to the sum of volatile components deduced from mineralogical data.

Fig. 4 shows the evolution of the XRPD patterns as a consequence of mineral transformations occurring in the original clay after thermal treatments up to 900 °C. At 400 °C the broad I-Sm interstratification band at around 5°2θ (d ~ 15 Å) moves toward higher angles due to the collapse of smectitic layers to about 10 Å caused by the loss of the in- terlayer water. At the same temperature, the disappearance of a small peak at about 4.18 Å corresponding to the main reflection of goethite is also observed. At 500 °C the basal kaolinite reflections disappear, ow- ing to the loss of crystallinity resulting from the dehydroxylation of the mineral, while small residues of the chlorite reflections are present up to 600 °C. Illite/muscovite reflections do not show changes (with exception of small relatively increasing intensity of (001) reflections due to superimposition of mica and shifted I-Sm reflections in conse- quence of interlayer water removal) up to 700 °C, when a small drop in the intensity of the (002) and (004) reflections can be observed. At 700 °C, a decreasing intensity of the calcite reflections is also observed,

Table 1
Bulk chemical (XRF) and mineralogical (XRPD) composition of LCR clay.

Chemical composition (wt%)				Mineralogical composition	
XRF		XRPD*		Mineral	Wt% (3σ)
SiO_2	35.67	SiO_2	39.9	Quartz	16.3 (0.7)
Al_2O_3	11.47	Al_2O_3	11.6	Calcite	31.2 (1.3)
CaO	21.15	CaO	19.9	Illite/Muscovite	3.8 (0.5)
K_2O	1.73	K_2O	2.8	R0 I(0.3)-Sm interstratification	24.5 (2.9)
Na_2O	0.34	Na_2O	0.4	Kaolinite	5.9 (1.0)
Fe_2O_3	6.67	Fe_2O_3	2.2	K-feldspar	4.2 (1.0)
MgO	1.91	MgO	2.0	Albite	3.2 (0.5)
MnO	0.15	MnO	–	Goethite	1.7 (0.2)
TiO_2	0.53	TiO_2	–	Dolomite	1.0 (0.2)
P_2O_5	0.07	P_2O_5	–	Chlorite	1.0 (0.3)
LOI	20.32	CO_2	13.7	Amorph	7.1 (6.3)
		H_2O	8.6	Tot_CM	35.2 (3.7)

* Calculated on the basis of mineral content estimated from Rietveld refinement. CM stands for clay minerals.

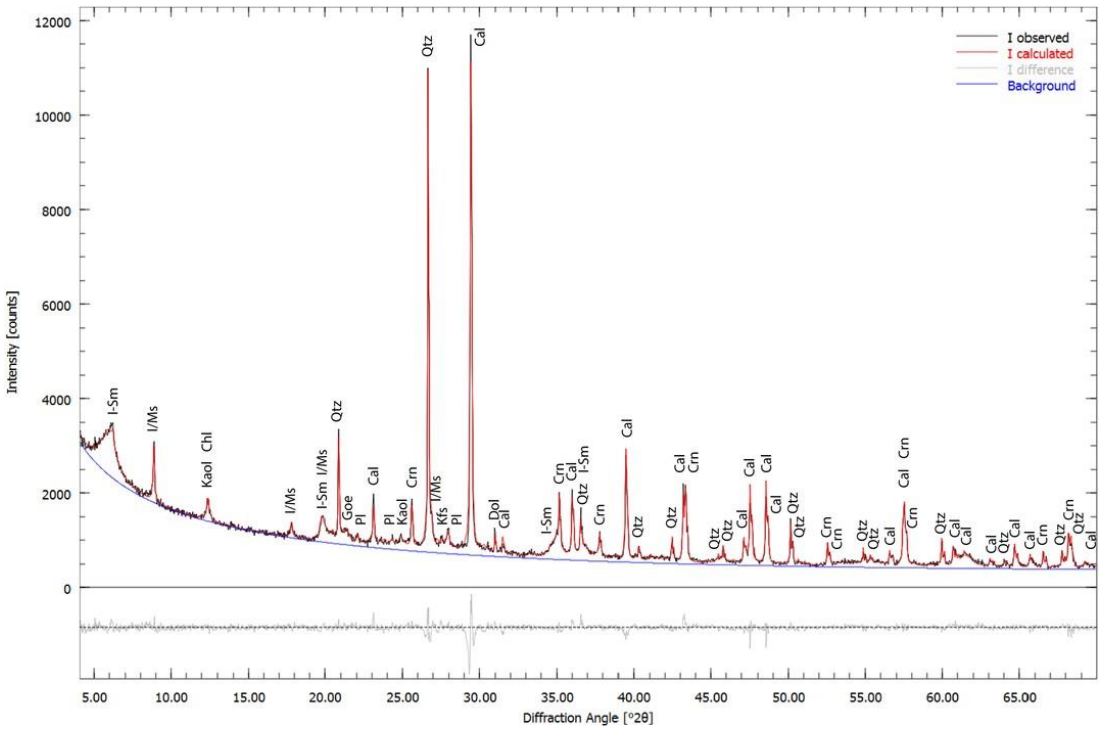

Fig. 3. Rietveld refined XRD pattern of LCR clay using BGMN program (*R*wp = 4.72%, *Rexp* = 3.13%). Mineral abbreviations: I-Sm = R0 illite-smectite interstratification with 30% illitic layers (R0 I(0.3)-Sm), I/Ms = illite/muscovite, Kaol = kaolinite, Chl = chlorite, Qtz = quartz, Goe = goethite, Crn = corundum, Pl = plagioclase, Cal = calcite, Kfs = K-feldspar, Dol = dolomite.

indicating the beginning of calcite decomposition, which results al- most completed at 800 °C. At this temperature, lime and traces of port- landite (due to lime rehydration) are detected in the samples together with anorthite and poorly crystalline Ca-silicate phases of the C_2S type, formed by the reaction of free lime, silica and alumina derived from decomposition of calcite and clay minerals (Allegretta et al. 2016; Letsch and Noll 1983; Riccardi et al., 1999). Ca-silicates together with poor crystallised hematite, form a broad band in correspondence of an angular interval of 32-35°2θ at 800 °C. At 900 °C, in coincidence with an abrupt decrease of the illite/muscovite reflections indicating the al- most complete breakdown of the mica structure (Cultrone et al. 2001; Guggenheim et al. 1987), an increase of new-formed and well-crystallised phases are observed, namely pyroxenes (diopside and wollastonite), gehlenite, Ca-olivine and hematite (Fig. 5). Calcination in reducing conditions did not show significant effects on the samples compared to oxidising ones, with the exception of a slightly higher stabilisation of calcite and, apparently, a delay in the formation of new Ca-silicate phases with respect to oxidising heating (Fig. 5).

XRPD patterns of clay samples ground for 5, 10, and 15 min show a general and gradual decrease of the characteristic reflection intensi- ties of clay minerals and calcite, associated with significant broaden- ing effects (Figs. 4b and 5). After 5 min of grinding, the band at ~ 5°2θ, where the basal reflections of I/Sm interstratifications and chlo- rite overlap, as well as the broad band at ~ 12.5°2θ, where (001) kaoli- nite and (002) chlorite reflections overlap, disappear, suggesting a significant degradation of the structure of these minerals. On the contrary, the main reflections of illite/muscovite are still present but showing a lower intensity and a higher broadening with respect to the original clay. After 10 and 15 min of grinding, the illite/muscovite basal reflec- tions become negligible, whereas non-basal reflections are still present although showing progressive decreasing intensity and an augmented broadening with the increase of grinding time. Among the non-clay minerals, the same effects of grinding on intensity and width can be observed on calcite main reflections as the treatment time is prolonged (Fig. 4b). It can be very well appreciated in Fig. 6, where the variation of intensity and Full-Width at Half-Maximum (FWHM) of the main calcite reflections after each treatment is displayed.

Quantitative estimation of the phase composition in mechanically treated clay samples shows yet after 5 min of grinding a significant decrease of calcite and illite-muscovite together with a progressive increase of the amorphous phase (up to 47 wt% after 15 min of grinding), mainly derived from the degradation of the crystal structures of the original clay material (Fig. 5).

The combination of mechanical and thermal treatment in both oxidising and reducing atmosphere caused only limited mineralogical modifications with respect to just ground samples up to a heating temperature of 500 °C (Fig. 4c). At 400 °C, only a small decrease of the background in the region from 4.5 and 7°2θ is observed, suggesting the persistence of relic I/Sm layers after the grinding, which are definitively lost after relatively low temperature heating. Furthermore, an increase in intensity and in the FWHM of the main reflections of calcite is observed up to the temperature of 500 °C, indicating a slight recrystallisation effect occurring during the first stage of heating, contrary to what observed in the just heated clay (Fig. 6). From 600 °C onwards, a progressive decrease of the calcite reflection intensities is shown with a trend proportional to the energy of grinding (i.e. from 600 to 700 °C the estimated calcite content decreases from 17 to 7 wt%, from 13 to 4 wt% and from 11 to 5 wt% in 5, 10 and 15 min mechanically pre-treated samples, respectively), whereas a complete disappearance of the mineral occurs at 800 °C in all samples. Instead, small residues of illite/ muscovite, which in samples ground for 10 and 15 min are represented only by non-basal reflections, remain almost unchanged up to 600 °C; at 700 °C, a significant decrease of the reflection intensity and related content of calcite is observed before its definitive disappearance occurring at 800 °C. X-ray pattern of quartz shows a slight decrease in intensity and an increase of the FWHM after heating at 600 °C samples pre-ground for 10 and 15 min, whereas heating from 800 °C to 900 °C

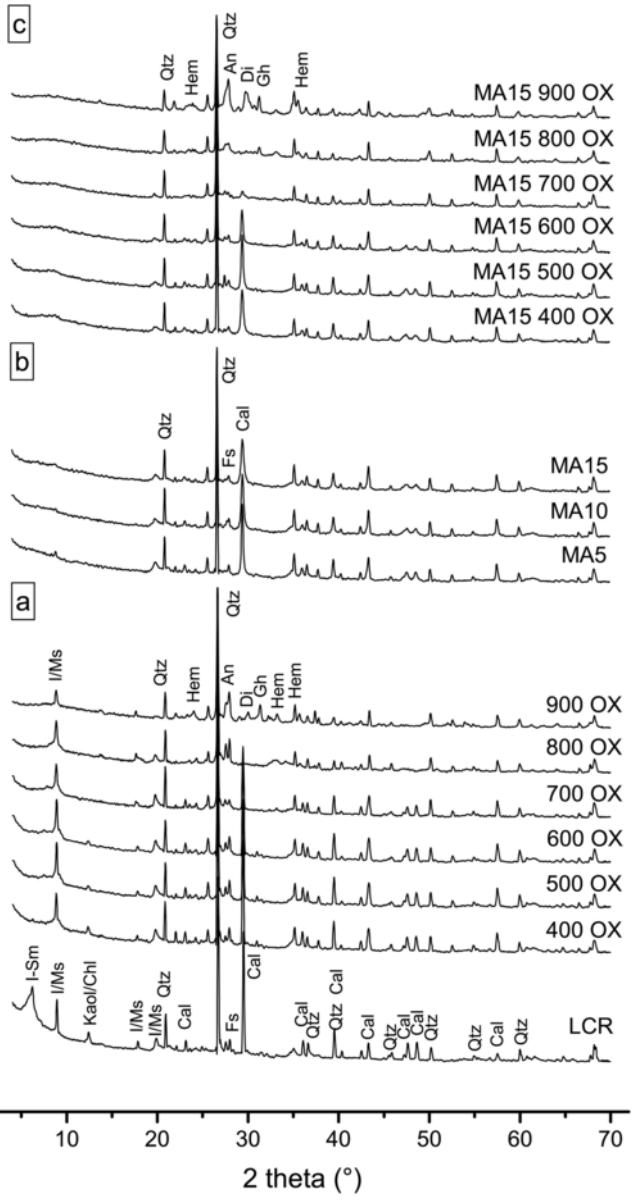

Fig. 4. XRPD spectra: a) LCR clay and thermal activation; b) mechanical activation; c) mechanical and thermal activation. Mineral abbreviations as in Fig. 3; Fs = feldspars, Di = diopside, Hem = hematite, Gh = ghelenite, An = anorthite.

causes a more significant decrease of the intensities and broadening of the quartz diffraction peaks in all mechanically and thermally treated samples. At 800 °C, a small band from 32.5 to 34°2θ associated to poorly crystalline Ca-silicates of the C_2S type, hematite, and traces of gehlenite forms in these samples. At the same heating temperature an increase of the reflection intensity and amount of plagioclase is also detected, but only in samples subjected to grinding for 10 and 15 min (Fig. 5). After heating at 900 °C, a diffraction peak corresponding to a more crystalline hematite occurs at around 33°2θ, combined with increasing intensities of the gehlenite reflections (in a lesser extent for 10-15 min ground samples) and additional crystalline anorthitic plagioclase and pyroxenes (diopside and wollastonite). Neither lime nor portlandite reflections are present in the X-ray powder pattern of samples heated after mechanical treatments. The amorphous phase content ranges around 40 wt% in samples heated up to 600 °C without significant variations with respect to the corresponding only ground sam- ple, then it increases from 700 to 800 °C and it decreases abruptly at 900 °C, in coincidence of the crystallisation of new phases. The maximum content of amorphous phase is observed at 800 °C for samples ground for 5 min (about 52 wt%) and at 700 °C for samples ground for 10 and 15 min. (about 54 wt%). Furthermore, the amount of the amorphous phase estimated in samples subjected to a combination of mechanical and thermal treatments is generally higher than that of just heated samples (Fig. 5). In analogy to observations done for the only calcined clay, the samples treated by a combination of mechanical and thermal processing showed a slight delay in the decomposition of calcite and a subsequent delay in the formation of new Ca-silicate phases when heated in almost reducing regime with respect to oxidising conditions. As a consequence of this deferment, the amorphous phase content is generally higher in samples subjected to high temperature heating in reducing atmosphere.

3.3. DTA/TG/DTG

DTA/TG/DTG analysis were performed on the untreated LCR clay and for comparison on the mechanically activated samples (MA5, MA10 and MA15), in order to evaluate the effects of high energy grinding on the thermal behaviour of minerals. The obtained results are reported in Fig. 7.

Three major weight-loss events are distinguishable in the unprocessed clay sample (Fig. 7a). In the first stage (< 300 °C), ther- mal dehydration takes place associated with the removal of water mol- ecules from various sorption sites in the clay structure (Heller-Kallai 2006) mainly ascribable to I-Sm interstratification. According to the TG curve, the main episode of dehydration is characterised by a marked weight-loss corresponding to a sharp peak at fairly low temperature (~ 65 °C) and a shoulder at about 130 °C in the DTG curve. At higher temperature, the TG curve declines very gradually and a second peak (~ 260 °C) is apparent in the derivative curve corresponding to a much smaller weight step. At higher temperature (> 300 °C) the sample dis- plays a second major weight loss as a result of dehydroxylation reac- tions of kaolinite and illite/muscovite and, to a lesser extent, of goethite (Gualtieri and Venturelli 1999). TG curve shows that kaolinite dehy- droxylation process starts slowly and increases gradually with a major water release at about 490 °C. In the last stage (> 600 °C) the thermo- gravimetric curve shows an abrupt rate decline up to about 760 °C, due to the decomposition of carbonates bringing to CO_2 release (Trindade et al. 2009) and residual dehydroxylation of smectite (Fernandez et al. 2011). At higher temperature the DTA curve continues monotonously until an exothermic peak is observed around 860 °C. The exothermic peak corresponds to the heat effect associated to the recrystallisation of decomposition products into more stable phases.

The mechanically activated samples are characterised by similar TG/DTG/DTA curves although the activation method has pronounced effects on the decline of thermogravimetric curve. A higher weight loss is observed for the 5 and 10 min mechanically treated samples com- pared to the unprocessed clay, in agreement with an enhanced particle surface area caused by grinding (Sánchez-Soto Wiewióra et al., 1997). Moreover, the three dehydration steps become more smoothed as the grinding time increases, and the sample weight loss decreases almost monotonically at the highest milling time, due to pronounced varia- tions in particle size with the increase of grinding treatment. The 15 min mechanically treated sample shows a lesser total weight loss, owing to the effect of a re-aggregation process that hampers the water diffusion (Sánchez-Soto Wiewióra et al., 1997).

The position, shape and broadness of peaks of the corresponding derivative curve are also affected as a function of the grinding time: the dehydration events are shifted to higher temperature, while the dehydroxylation reaction of clays and the carbonates decomposition process are shifted to lower temperature (Balek et al. 2007). The increase in

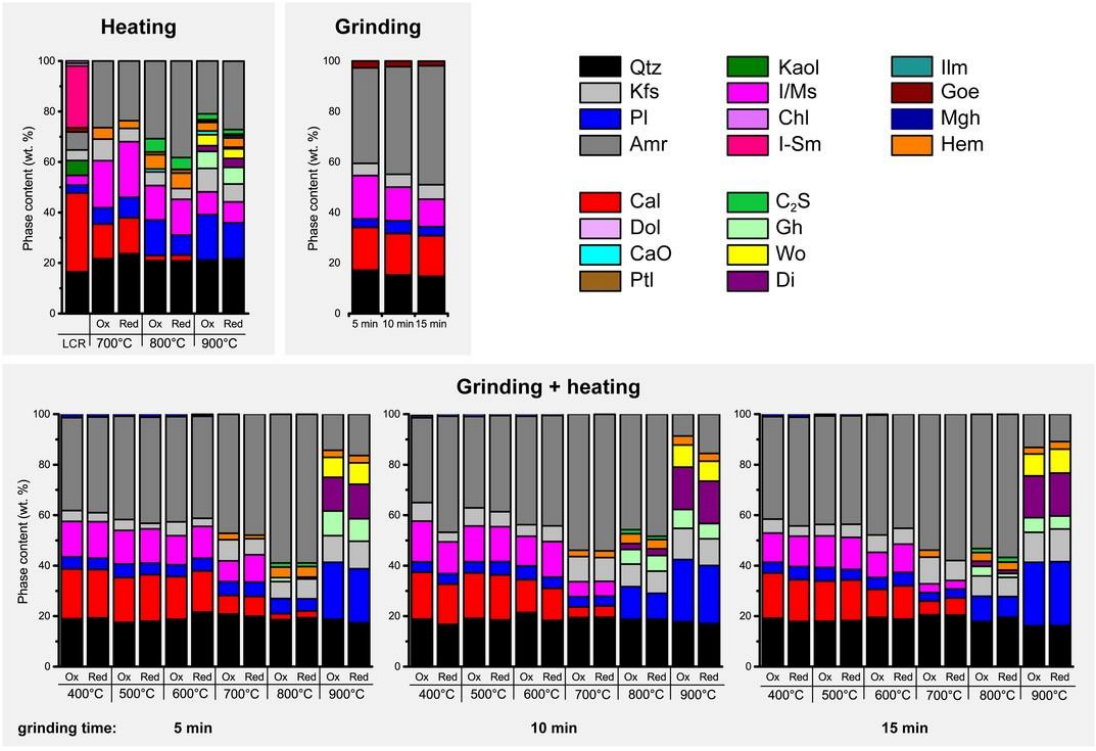

Fig. 5. Block diagram of mineralogical evolution after activation treatments by XRPD. Mineral abbreviations as in Figs. 3 and 4; CaO = lime, Ptl = portlandite, Ilm = ilmenite, Mgh = maghemite, Kfs = K-feldspar, Wo = wollastonite, C_2S = bi-calcium silicates, Amr = amorph.

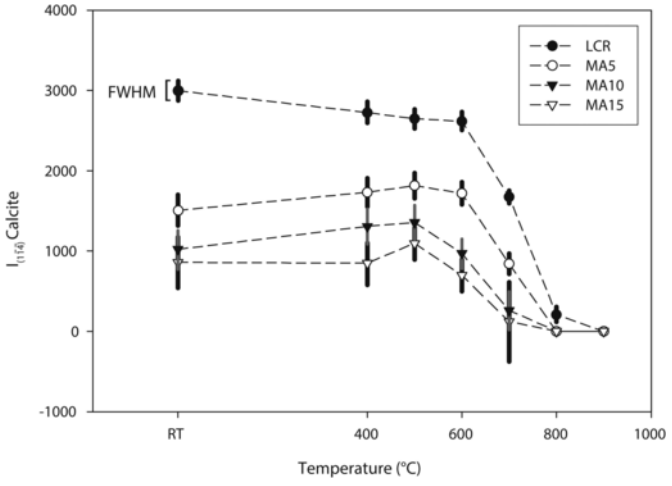

Fig. 6. Intensity and Full-Width at Half-Maximum (FWHM) of the main calcite reflection (1-1-4) at room temperature (RT) and after thermal treatment (from room temperature to 900 °C), mechanical activation (MA5 = 5 min grinding, MA10 = 10 min grinding, MA15 = 15 min grinding) and combination of mechanical and subsequent thermal treatments. The FWHM is represented by vertical lines sample symbols.

DTG dehydration peak temperatures is attributed to the particle tight packing as a consequence of the reduction of sample size with grinding The shift of dehydroxylation events at lower temperature is related to the structural modification due to exfoliation and the removal of the OH groups by mechanical treatment (Sánchez-Soto et al. 1994; Balek et al. 2007). Lower temperatures of carbonates decomposition were also associated with the increase of specific surface area of treated samples due to a decrease in particle size. The exothermic DTA effects of new formed phases are consequently shifted to lower temperatures with the increase of grinding time.

3.4. FTIR

The FTIR analyses were performed on a selection of samples which, on the basis of XRPD and DTA/TG/DTG results, have shown marked clay mineral decomposition after mechanical and/or thermal activation treatments to be considered the most suitable precursors for alkaline activation. In particular, the selected samples were: thermally treated samples at 800 °C in both oxidant and reducing atmosphere (samples 800 OX, 800 RED); high energy ground samples for 10 and 15 min, respectively (samples MA10 and MA15); samples subjected to high energy grinding for 10 and 15 min followed by heating at 700 °C in both ox/red conditions (samples MA10 700 OX, MA10 700 RED, MA15 700 OX, MA15 700 RED).

FTIR data of samples activated by different methods are reported in Fig. 8 in comparison with that of the unprocessed raw material (LCR). The FTIR spectrum of the untreated material is dominated by the characteristic vibration bands of clay minerals (illite/muscovite, I-Sm interstratification, kaolinite), quartz and carbonates (mainly in the form of calcite), in agreement with XRPD results. The band at 3697 cm^{-1} is specific to kaolinite hydroxyl groups (Vaculíková and Plevová 2005) and is related to the in-phase symmetric stretching vibra- tions of OH groups located at the octahedral surface, which are weakly linked through hydrogen bonds to the Si-O-Si group oxygens of the adjacent layer (Madejová 2003). The absorption band near 3620 cm^{-1} is attributed to hydroxyl groups which are located between the tetra- hedral and octahedral sheets of phyllosilicates, usually found in prin- cipal clay-minerals (Madejová 2003). The broad absorption band cen- tred at 3421 cm^{-1} is characteristic of OH stretching vibrations of phyllosilicates with some adsorbed/interlayer water. Indeed this broad band appears reduced after the sample was heated overnight. The band at 1635 cm^{-1} is the corresponding bending vibration of H-O-H groups in interlayer/adsorbed water molecules (Srasra et al. 1994; Tyagi et al. 2006; Yu et al. 1999). The intensive band peak at 1033 cm^{-1} is as

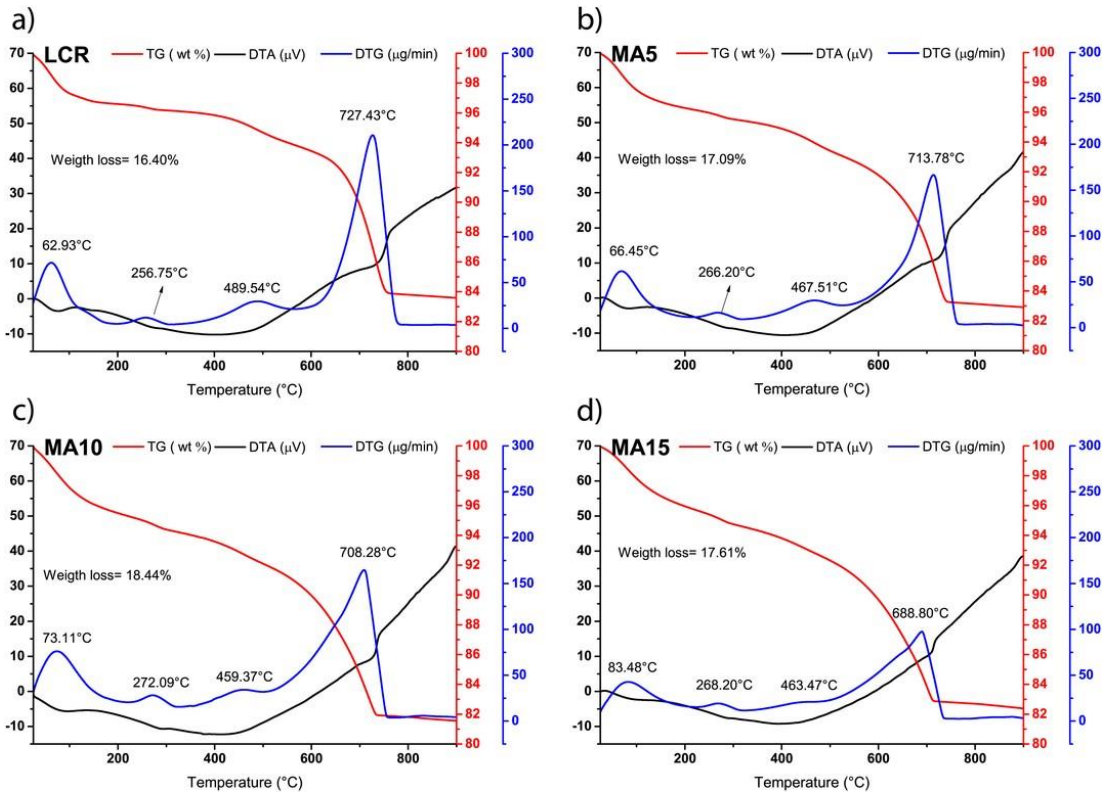

Fig. 7. DTA/TG/DTG curves of unprocessed LCR clay (a) and clays ground for 5 (b), 10 (c) and 15 (d) minutes.

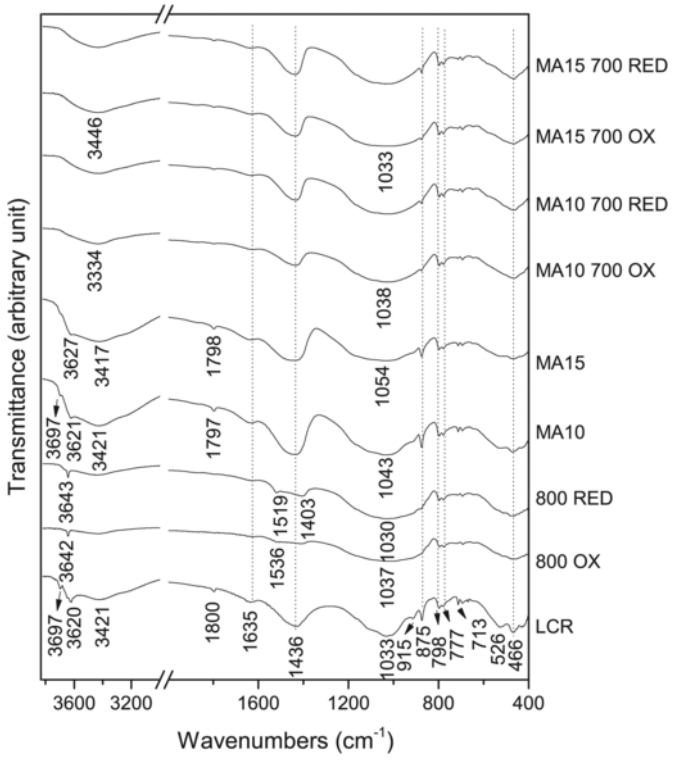

Fig. 8. FTIR spectra from bottom to top: unprocessed clay (LCR); clay samples thermally treated at 800 °C in oxidising and reducing atmosphere (800 OX and 800 RED); clay samples mechanically treated for 10 (MA10) and 15 min (MA15); clay samples mechanically treated for 10 and 15 min and subsequently heated at 700 °C in oxidising and reducing atmosphere (MA10 700 OX, MA10 700 RED, MA15 700 OX and MA15 700 RED).

signed to Si-O in-plane stretching of illite (Vaculíková and Plevová 2005), kaolinite (Aglietti et al. 1986) and montmorillonite (Madejová 2003; Tyagi et al. 2006) minerals, whereas the shoulder at about 1110 cm^{-1} corresponds to the out of plane Si-O symmetrical stretch- ing vibration (Ferone et al. 2015). The bands at about 526 and 470 cm^{-1} are associated respectively to Si-O-Al and Si-O-Si bending vibrations (Madejová 2003) in silicate phases. More or less intensive bands are caused by presence of calcite ($CaCO_3$) at 1426, 1800, 875 and 713 cm^{-1}.

The IR spectrum of the clays mechanically activated for 10 and 15 min does not show relevant changes compared to that of the unprocessed sample. In particular, a progressive intensity decrease of the OH stretching bands of illite/muscovite and kaolinite as well as the Al-OH inner hydroxyl deformation vibration of kaolinite is observed as the mechanical activation is performed for longer time. This is due to significant changes in the surface structure of these phyllosilicate at the molecular level as a consequence of the mechanical treatment. Indeed, mechanical treatment supplies sufficient energy to break the hydroxyl bonds between adjacent phyllosilicate layers.

The relative intensities of the absorption bands associated to quartz and calcite remain almost constant upon grinding whereas a broadening of the Si-O-T stretching band centred at 1043 cm^{-1} is observed, testifying the occurrence of stacking disorder involving phyllosilicates.

From FTIR spectra the significant effect exerted by thermal treatments on samples is evident, resulting mainly in a modification of the characteristic bands of clay minerals and carbonates (Chukanov 2014). In particular, the heating at 800 °C is responsible for the almost complete dehydroxylation of clay minerals, as shown by the quite complete disappearance of the -OH stretching bands at 3698 and 3620 cm^{-1} (Srasra et al. 1994). Moreover, the thermal treatments at 800 °C in both oxidising and reducing regimes have the effect to induce also a decrease in the intensities of the Al-OH and Si-O-Al bending vibration bands, respectively at 915 cm^{-1} and at about 526 cm^{-1}, as a conse

quence of the dehydroxylation process and the structural disruption of the phyllosilicate sheets (Madejová 2003). Additionally, the calcite characteristic bands at 2875, 1800, 875 and 713 cm^{-1} are almost disappeared. The small bands between 1520 and 1400 cm^{-1} are due to vibration modes of CO_3^{2-} groups and are most probably ascribable to residues of carbonates. The almost complete decomposition of carbonates is most pronounced in the case of sample heating at 800 °C in oxidising regime with respect to the reducing one. The concomitant appearance of the OH stretching band at 3640 cm^{-1} is due to portlandite ($CaOH_2$) as the reaction product of CaO (from calcite decarbonation) with atmospheric water vapour (Ferone et al. 2015).

The combination of mechanical (10 min and 15 min) and thermal (700 °C OX) treatments on clay brings to the almost complete clay mineral structural decomposition, as proved by the disappearance of the OH stretching vibrations of structural hydroxyls at 3698 cm^{-1}, and of the band centred at 3620 cm^{-1} (OH stretching of inner hydroxyl groups) and at about 913 cm^{-1} (OH deformation of inner hydroxyl groups) (Souri et al. 2015). The complete disappearance of the Al-O-Si band (at about 526 cm^{-1}) is the effect of structural disruption in the bonds between tetrahedral and octahedral sheets of clay minerals (Aglietti et al. 1986; Vizcayno et al. 2010). The very broad and less featured Si–O stretching band centred at 1038 cm^{-1} point out to an enhanced structural disorder of silicates (Tyagi et al. 2006; Vizcayno et al. 2010).

There is no noteworthy difference between the heat treatments in different burning regimes, except for carbonates. Indeed, the less intense characteristic bands at 1437 and 875 cm^{-1} point out to a higher extent of calcite decomposition in oxidising regime.

In general, all the treatments have a negligible effect on quartz (Souri et al. 2015), whose persistence is indicated by the characteristic bands at 798, 779 and 694 cm^{-1} (Tyagi et al. 2006) for all treated sam- ples.

3.5. Leaching test

The solubility tests in a 3 M NaOH were performed on the same samples selected for FTIR investigations, which showed the highest extent of clay mineral decomposition and thus highest amorphous phase content, to be considered the most suitable precursors for alkali activation.

The solubility test showed that the release of Al and Si increases with the grinding time and it is favoured at lower temperature (700 °C) in the case of combination of mechanical and thermal treatments, compared to just heated samples (Table 2). The soluble Si/Al ratio is above 3 in the untreated raw clay material, while it ranges from 1 to 2 in the treated clays, due to the increase of Al leaching from the low crystalline-amorphous silicates. Calcium shows a general very low solubility in alkaline solutions as already observed in literature (García-Lodeiro et al. 2013), although a slight increase was observed in clays heated at 800 °C. The highest K leaching was obtained from clays ground at 30 Hz for 10 and 15 min.

The highest absolute release of soluble species (sum of Al, Si, Ca and K) in leachates has been observed for mechanically/thermally treated samples, followed in order of abundance by mechanically treated samples, whereas the lowest values are observed for the thermally treated samples (Table 2). The overall Si/Al ratio detected for the samples subjected to a combination of mechanical and thermal treatments is about 1, whereas it increases after thermal or high energy grinding treatment alone, as a consequence of a lower extent of Al solubility from less reactive clay minerals. The reducing burning regime adopted during the heating of the mechanically treated samples seems not to enhance the clay reactivity and thus the solubility of species in alkaline medium, whereas the solubility of Al and K is enhanced by the adoption of the reduced burning regime in the case of the thermally treated samples, as observed in literature (Seiffarth, et al., 2013).

4. Evaluation of the activation methods

It is known that the soluble Si/Al ratio in the starting material composition affects the setting and hardening times of the derived geopolymers (De Silva et al. 2007). Low Si/Al values will accelerate setting and hardening. Besides, a Si/Al ratio between 2 and 3 from starting materials could ensure a good potential for the synthesis of alkali activated materials (Seiffarth, et al., 2013). In our case, the soluble Si/Al ratio after dissolution tests in 3 M NaOH ranges from 1.0 to 1.7, regardless of the type of treatment: mechanical, thermal or both. This value is clearly lower than the theoretical Si/Al ratio of the raw clay (i.e. 2.78) due to the presence of non-reactive and poorly soluble crystalline phases (e.g. quartz) in the clay.

In Fig. 9a the soluble Si and Al (in ppm) in the 3 M NaOH solu- tion are plotted together with the amorphous phase content and crys- talline phases as determined by quantitative XRPD. The lowest Si and Al solubility was observed for the samples heated at 800 °C, which are those with the highest soluble Si/Al ratio (Table 2). This is consequence of the major preservation of clay mineral structures (illite/muscovite in particular) during the thermal treatment with respect to the other activation methods. The lowest K solubility in the heated samples can be related to the same effect (Fig. 9b). Instead, the different Si/Al ra- tio and the slight variation in Ca solubility observed between 800 OX and 800 RED samples can be due to the diverse stability of clays min- erals and calcite during heating in different burning regimes and to the consequent variation in the content of non-stoichiometric poorly crystalline Ca-silicates and -aluminosilicates formed as precursors of equilibrium phases, i.e. anorthite and diopsidic pyroxene (Riccardi et al. 1999), not observed in samples subjected to other treatments. As a consequence, the 800 RED sample shows minor new formed plagioclase (less soluble) and higher amorphous phase content (more soluble) than the samples heated under oxidising condition, which can likely explain the observed increase of Al solubility. This evidence, together with the

Table 2
Release of Si, Al, K and Ca (ppm) from the selected clays in 3 M NaOH solution.

	Sample	Si	Al	K	Ca	*Total	Si/Al
Original (reference)	Theoretical	–	–	–	–	–	2.78
	LCR	88.93	26.04	31.05	45.66	191.68	3.42
Mechanical activation	MA10	294.43	237.38	242.02	22.32	796.15	1.24
	MA15	555.37	497.11	303.82	6.32	1362.62	1.12
Thermal activation	800 OX	305.10	181.17	51.98	22.70	560.95	1.68
	800 RED	356.37	309.83	67.32	21.88	755.40	1.15
Mechanical activation + thermal activation	MA10 700 OX	744.56	705.37	143.51	7.30	1600.74	1.06
	MA10 700 RED	661.61	642.05	123.55	6.44	1433.65	1.03
	MA15 700 OX	694.25	663.82	147.91	6.19	1512.17	1.05
	MA15 700 RED	683.01	677.88	141.89	6.22	1509.00	1.01

* Total = [Al] + [Si] + [K] + [Ca].

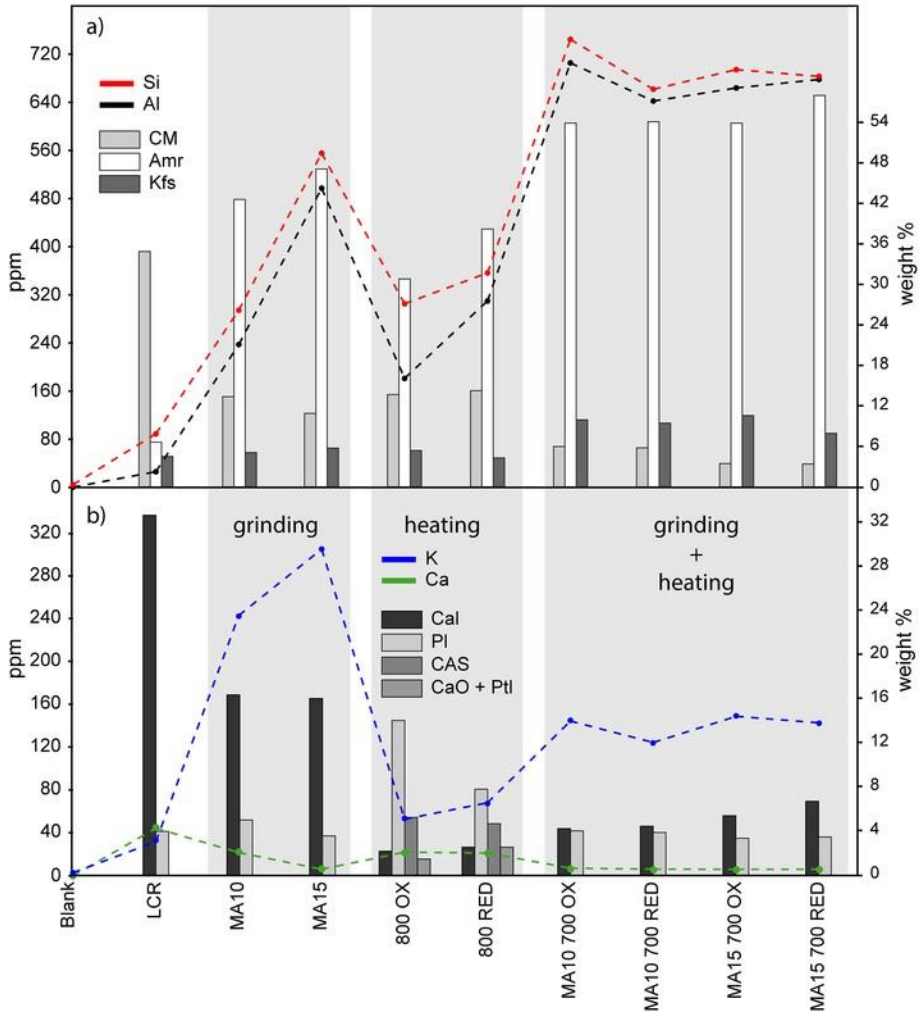

Fig. 9. Solubility trends and principal phases variability of: unprocessed clay (LCR); clay samples mechanically treated for 10 (MA10) and 15 min (MA15); clay samples thermally treated at 800 °C in oxidising and reducing atmosphere (800 OX and 800 RED); clay samples mechanically treated for 10 and 15 min and subsequently heated at 700 °C in oxidising and reducing atmosphere (MA10 700 OX, MA10 700 RED, MA15 700 OX and MA15 700 RED). Mineral abbreviations: CM = total clay minerals, Amr = amorph, Kfs = K-feldspar, Cal = calcite, Pl = plagioclase, CAS = Ca-aluminosilicates, CaO = lime, Ptl = portlandite.

almost similar percentages of illite/muscovite in both 800 RED and 800 OX samples, suggests that increasing amorphous phase content (and thus Al leaching) in 800 RED samples is not related to an intensification of dehydroxylation of clay minerals under reducing heating conditions, contrary to what observed in Seiffarth et al. (2013) for illitic non-calcareous clays. Thus, in our carbonate-rich clay the onset of mineralogical reactions between clay minerals and calcite have changed their respective thermal stability.

XRPD and FTIR clearly show that the mechanical process resulted in a progressive loss of crystallinity of minerals and reduction of their crystal size. It was observed that a mechanical activation treatment performed for 10 min can promote the amorphisation of clay minerals, bringing to an illite/muscovite content comparable with that obtained after clay calcination at 800 °C, but with a less extent of calcite decomposition and without the formation of poorly reactive Ca-aluminosilicate phases promoted by the heat treatment. Furthermore, the intensities of the general (hkl) reflections of illite/muscovite decrease less than those of the basal (00l) reflections after mechanical treatments, suggesting delamination effects occurring during grinding, produced by the progressive loss of periodicity perpendicularly to the layer plane and to the reduction of dimension along the c direction, leading to too small sized crystallites to produce coherent scattering (Sánchez-Soto et al., 2000). As shown by reactivity test (Fig. 9a), the Si and Al solubility in NaOH of samples ground for 10 min is almost similar to that of the thermally treated samples at 800 °C, although with a slight different Si/Al ratio. However, a very high value of K release is observed in ground sample leachates, mainly related to the delamination occurring within 2:1 layer silicates. The intensification of grinding caused more significant degradation effects on clay mineral structures and on calcite, which are not clearly shown from X-ray diffraction patterns but can be well detected by the intensity reduction of the OH stretching bands in FTIR diagrams (Fig. 8). DTA/TG/DTG analysis also showed that grinding affected significantly the thermal behaviour of the clay minerals, as it can be derived from mass loss profiles (Fig. 5). The decrease of par- ticle size fosters their tight packing so hindering the water diffusion through the clay minerals and causing the shift toward higher temper- atures of their dehydration. Moreover, we suppose that higher surface area of particles produced by exfoliation by grinding made the clay min- eral layers less stable and facilitated at lower temperature the removal of OH groups (Figs. 5 and 6). In addition, higher surface areas pro- duced by the decreasing particle size after the grinding favoured the reaction involving the OH groups during heating and the progressive elimination of structural water. The significant increase of Al and Si solubility in the sample ground for 15 min can be thus clearly related to the incipient rupture of bonds in tetrahedral and octahedral sheets during grinding, while the slight increase of K solubility may be due to

late delamination effects on coarser muscovite relics. The mechanical activation caused only size reduction on calcite and no decomposition or polymorphic transformations (Pesenti et al. 2008) were detected. The progressive decrease of Ca solubility in mechanically activated clays is (inversely) correlated with the grinding time and with the Si, Al and K solubility but not with calcite amounts, although the significant decrease of calcite crystals during grinding (Fig. 7). Furthermore, the Ca solubility is similar to that of Si, Al and K in the untreated clay, while in ground samples the solubility of Si, Al and K increases of an order of magnitude and that of Ca decreases to a quarter (i.e. sample MA15, Fig. 9). On the other hand, the soluble Si/Al ratio in the ground clay is one third of the untreated clay (Table 2). Such dissolution trends may be explained taking into account the different hardness of minerals (calcite and tectosilicates versus clay minerals) and therefore their behaviour during grinding. It is our opinion that agglomeration of particles from the extensive amorphisation of clay minerals may have created coating effects on harder calcite grains, so inhibiting its dissolution under our experimental conditions.

Combination of mechanical and thermal treatment caused higher structural changes in the clay, resulting in a general anticipation of the illite/muscovite breakdown of about 200 °C with respect to the just heated sample (Fig. 5) and significant decomposition effects on calcite at already 700 °C (Fig. 6), with a subsequent increase of the total amorphous phase detected from XRPD. Moreover, the combination of the two activation methods anticipated of about 100 °C the formation of Ca-silicates (anorthite, gehlenite and diopside) and the content of such new formed phases were higher in ground samples heated at 800 and 900 °C under oxidising conditions compared to reducing burning. This can be likely explained as a combined effects of grinding, enhancing decomposition reactions, with the partial stabilisation of calcite in reducing atmosphere, which is known to inhibit the formation of calcium-aluminosilicates (Letsch and Noll 1983).

From Fig. 9 it can be seen that the selected clay samples treated by the combination of the two methods (MA10 700 OX/RED, MA15 700 OX/RED) show the highest amorphous phase contents and a slight increase of K-feldspar compared to the unprocessed clay. A significant decrease of calcite content is also observed from X-ray QPA analyses (Figs. 5 and 9), but not confirmed from FTIR data (Fig. 8), showing characteristic vibration bands associated to carbonate bonds (Galván-Ruiz et al. 2009). The occurrence of such calcite relics can at the same time explain the absence of lime, Ca-silicates and -aluminosilicates in ground samples heated at 700 °C. The coupled reactions of decomposition of both clay minerals and calcite, which characterises the only heated samples (Fig. 5), occurred separately in samples subjected to the combination of treatments. In the latter case, the more rapid decomposition of clay minerals favoured the nucleation of K-feldspars in the illite/muscovite relic domains during heating. In other words, when the activity of Si and Al is high (decomposition of clay minerals), that of Ca is low (calcite still stable) and hinders the formation of Ca-silicates and -aluminosilicates (Figs. 5, 9). Samples ground for 10 and 15 min. and heated at 700 °C showed the highest release of Si and Al in alkaline solution, which can be greatly related to their highest amorphous phase content (Fig. 9), thus showing that the treatments bringing to the major extent of mineral decomposition are the most effective in increasing the clay reactivity for the alkali activation purpose. Contrary to what observed in only heated samples, the Si and Al dissolution behaviour of mechanically and thermally treated samples does not show noticeable differences between the two different burning regimes.

Summarising, the three activation procedures here applied on illite carbonate-rich clay provided silico-alluminate systems with variable degree of amorphisation and a different content and crystallinity of mineral phases. Note that the amorphous phase detected from XRPD occurs in the samples in different form: in the case of mechanical activated samples it results from significant crystal size decrease and delamination effects, while in the case of thermally treated samples and in samples subjected to the combination of mechanical and thermal activation, dehydroxylation/decomposition phenomena occur, fostering the formation of new crystalline phases. The disruption of crystal structures through dry grinding is responsible for the anticipation of phase transformations during subsequent clay heating and for lowering the temperature range coinciding with the highest clay amorphous phase content. DTA/TG/DTG analysis of mechanically treated samples shows the gradual shift of the DTG peak falling at about 730 °C toward lower temperatures and the increase of the peak asymmetry, as a consequence of the progressive size reduction of carbonates and the residual dehydroxylation of 2:1 clay minerals. The different structural modification modes of clay minerals under the selected activation methods result in different leaching of Si and Al in alkaline solution, rather than in a variation of their ratio (Table 2). The soluble Si/Al ratios above 1 found for all treated samples accounts for almost complete decomposition from prevailing 2:1 clay minerals. Late dehydroxilation effects on 2:1 clay minerals are observed from 700 to 950 °C due to OH groups bonded in Al (Mg) octahedra sandwiched between silica tetrahedra, more resistant to decomposition. The occurrence of extensive disruption of the phyllosilicate sheets is well accounted in samples activated by the combination of mechanical and thermal treatment from FTIR data, showing the disappearance of the characteristic Al-OH and Si-O-Al bending vibration bands at 915 cm^{-1} and at about 526 cm^{-1} respectively (Madejová 2003), and the substitution of the structural OH vibration bands of phyllosilicates with a broad band (3440 cm^{-1}) associated to the stretching vibration OH groups from adsorbed and interlayer water (Souri et al. 2015; Vizcayno et al. 2010).

One of the main aspects of the clays here studied is the role played by mineral species that bring Ca. Other than the different nature and amounts of amorphous phase, the three activation procedures bring Ca in different forms: 1) calcite; 2) Ca-silicates and -aluminosilicates; 3) amorph. Recent works focusing on the reaction products of hybrid cements propose models for the formation of C-A-S-H and N-A-S-H phases and show that the stabilisation of these phases depend mainly by the Ca concentration and the pH of the activator solution (García-Lodeiro et al. 2010, 2011, 2013). Khater (2012) reports that the addition of $Ca(OH)_2$ up to 10 wt% to the starting aluminosilicate resources improves the mechanical strength of geopolymers, thanks to the diffused nucleation of C-S-H, which contributes to form a homogeneous and fine microstructure. An increase of the compressive strength of geopolymers was also observed by Yip & Van Deventer (2002), which found that samples prepared with an amorphous source of Ca activated with low concentrated sodium hydroxide solutions worked better than those derived from the activation in the same pH conditions of a blend with a crystalline source of Ca. The original presence of calcite in our raw clay gives the opportunity to use Ca-bearing phases already present in the starting material.

The mineral associations produced from the three treatment types on the carbonate-rich clays gave a complex mixture of relics and new formed phases which can interact differently with alkali solutions. The behaviour of each mineral assemblage in alkali solutions is not easily predictable and specific tests changing pH and time of curing are necessary. Chemical micro-domains may direct the precipitation of different gels according to the local activity of Si, Al, Ca and K available during alkaline activation. However, some general considerations can be made here. The samples heated at 800 °C show the highest soluble Si/ Al ratio, as well as the highest Ca and lowest K solubility in alkaline medium. However, the absolute values of soluble species observed in leachates are the lowest among the differently treated samples. Reducing burning regime adopted during clay heating do not contribute significantly to the enhancement of clay mineral decomposition and thus on the clay reactivity as expected from literature results (Seiffarth et al., 2013). The samples ground for 10 min produce Si, Al and Ca solu

bility in alkaline solution similar to those of heated samples and may represent a cheaper equivalent, although the nature of amorphous phase is different. The combination of mechanical and thermal treatment at 700 °C gives a very high amorphous phase content, with the highest leaching of Si and Al in the 3 M NaOH solution. It can be supposed that better compressive strengths can be obtained for these samples owing to the high availability of Al and Si, which enhances the extent of polymerisation reactions. Also in this case, the heating in different regimes did not produce significant effects on mineral decompositions and clay reactivity.

On the basis of the effects of different treatments on carbonate-rich illite clay reactivity here discussed we considered the 10 and 15 min ground samples (MA10 and MA15) and the samples subjected to 10 and 15 min grinding and subsequent heating at 700 °C (MA10 700OX and MA15 700OX) as the most potentially reactive materials to be involved in the production of alkali activated binders. These samples have been thus selected for synthesis experiments reported in D'Elia et al. (in prep.), aiming to the investigation of factors influencing alkali activation and resulting strengths of products from these activated clays. As a matter of fact, although low Ca releases are observed in all of these activation conditions, the reaction pathways during alkaline activation could be strongly influenced by the kind and concentration of the activator. It is known that, for low concentrations of the alkaline activator, the gels formed in the first stages of the geopolymerization reactions lead to a decrease of the solution pH and to a subsequent increase in dissolution of calcium compounds (Alonso and Palomo 2001). The choice of this kind of precursors represents a novelty in the field of alkali activated binder productions, as to date the use of similar carbonate-bearing clays for geopolymeric purpose were solely attempted by Ferone and coworkers (Ferone et al. 2013, 2015), but in that case only thermally activation was explored and good mechanical performances of geopolymeric products were obtained only by using a sodium silicate solution and ground blast furnace slag.

5. Conclusions

Our results about three modes of activation of a carbonate-rich clay - mechanical, thermal and mechanothermal - show that amorphisation occurs in all the samples with a different extent. The activated samples with the highest content of amorphous phase were further analysed by FTIR and underwent leaching tests in a 3 M NaOH solution. The application of the three processing routines yielded three different types of activated clays, showing different leaching behaviours:

1) high energy grinding preferentially amorphises clay minerals and calcite, even though Ca solubility in alkaline solution is low. A two-step process of decomposition was outlined in the ground clays. The first step is characterised by incipient delamination of sheet silicates with significant K leaching from illite/muscovite (Si/K ≈1:1), while the second step consists of structural damages of 1:1 and 2:1 layers with significant increase of Si and Al release (Si/Al ≈ 1:1, Si/K ≈ 2:1).

2) samples subjected to heating at 800 °C show the highest soluble Si/Al ratio (≈ 1.7) among the different treated samples, but the Si and Al absolute concentration in leachates are equal or lower than those obtained from ground clays. Partial dehydroxylation of clay minerals accounts for this. Relative higher leaching of Ca may be due to scarcely crystalline Ca-silicates and -alumosilicates and portlandite solubilisation. The heating in different atmosphere (oxidising or mild reducing) influences the decomposition of calcite and, subsequently, the temperature to which the crystallisation of new Ca-silicates (gehlenite, anorthite and poorly crystalline C_2S phases) occur, which is higher in the case of reducing burning. This greatly influences the release of Al in the samples.

3) high energy grinding and heating at 700 °C yields an extended amorphisation, which leads to the highest leaching of Si and Al (Si/K = 1:1) and the lowest of Ca. More generally, it was shown that the combination of mechanical and thermal treatments anticipates the breakdown of clay minerals of about 200 °C with respect to just thermal activation. The heating in different atmospheres causes similar effects, although less evident, than those observed in solely heated samples.

These findings represent an important starting point for a better understanding of the mechanisms involving Apulian carbonate-rich clays with regard to different treatments promoting their reactivity and to exploit the potential of such poorly studied, widely available and cheap precursor to be involved in the production of green binders after the optimisation of sustainable procedures, with derived economic and environmental benefits.

To sum up, carbonate-rich clays are cheap and versatile raw materials for industry of innovative binders according to a properly selected activation method. However, the complexity of the obtained activated clays requires a deep knowledge of all involved parameters (i.e. activator concentration, curing conditions) to fully understand their real exportability to the industry. The influence of these parameters were carefully investigated in the out coming paper by D'Elia et al. (in prep.).

Acknowledgements

We thank Saverio Fiore, Emanuela Schingaro, Annarosa Mangone and Mauro Pallara for their help and scientific support. This work beneficed of instrumental upgrades of Potenziamento Strutturale PON-a3_00369 dell'Università degli Studi di Bari "A. Moro" titled "Laboratorio per lo Sviluppo Integrato delle Scienze e delle TEcnologie dei Materiali Avanzati e per dispositivi innovativi (SISTEMA)". This study is part of the Ph.D thesis by A.D. financed by the University of Bari, Italy.

References

Aglietti, E.F., Porto Lopez, J.M., Pereira, E., 1986. Mechanochemical effects in kaolinite grinding. I. Textural and physicochemical aspects. Int. J. Miner. Process. 16, 125–133.

Allegretta, I., Pinto, D., Eramo, G., 2016, 223–234.. Effects of grain size on the reactivity of limestone temper in a kaolinitic clay. Appl. Clay Sci.

Alonso, S., Palomo, A., 2001. Alkaline activation of metakaolin and calcium hydroxide mixtures: influence of temperature, activator concentration and solids ratio. Mater. Lett. 47, 55–62.

Bakharev, T., 2005. Resistance of geopolymer materials to acid attack. Cem. Concr. Res. 35, 658–670.

Baláž, P., 2003. Mechanical activation in hydrometallurgy. Int. J. Miner. Process. 72, 341–354.

Balek, V., Pérez-Maqueda, L.A., Poyato, J., Černý, Z., Ramírez-Valle, V., Buntseva, I.M., Pérez-Rodríguez, J.L., 2007. Effect of grinding on thermal reactivity of ceramic clay minerals. J. Therm. Anal. Calorim. 88, 87–91.

Barbosa, V.F.F., MacKenzie, K.J.D., Thaumaturgo, C., 2000. Synthesis and characterisation of materials based on inorganic polymers of alumina and silica: sodium polysialate polymers. Int. J. Inorg. Mater. 2, 309–317.

Bauluz, B., Mayayo, M.J., Fernández-Nieto, C., Cultrone, G., González López, J.M., 2003. Assessment of technological properties of calcareous and non-calcareous clays used for the brick-making industry of Zaragoza (Spain). Appl. Clay Sci. 24, 121–126.

Bergmann, J., Friedel, P., Kleeberg, R., 1998. BGMN-A new fundamental parameters based Rietveld program for laboratory X-ray sources, it's use in quantitative analysis and structure investigations. CPD Newsl. 20, 5–8.

Buchwald, A., 2006. What are geopolymers? Current state of research and technology, the opportunities they offer, and their significance for the precast industry. Betonw. Fert. Precast. Plant Technol. 72, 42–49.

Buchwald, A., Hohmann, M., Posern, K., Brendler, E., 2009. The suitability of thermally activated illite/smectite clay as raw material for geopolymer binders. Appl. Clay Sci. 46, 300–304.

Carretero, M.I., Dondi, M., Fabbri, B., Raimondo, M., 2002. The influence of shaping and firing technology on ceramic properties of calcareous and non-calcareous illitic-chloritic clays. Appl. Clay Sci. 20, 301–306.

Cheng, T.W., Chiu, J.P., 2003. Fire-resistant geopolymer produce by granulated blast furnace slag. Miner. Eng. 16, 205–210.

Chukanov, N.V., 2014. Infrared spectra of mineral species: extended library. In: Springer Geochemistry/Mineralogy. Springer, Netherlands, Dordrecht.

Cultrone, G., Rodriguez-Navarro, C., Sebastian, E., Cazalla, O., De La Torre, M.J., 2001. Carbonate and silicate phase reactions during ceramic firing. Eur. J. Mineral. 13, 621–634.

Davidovits, J., 1991. Geopolymers: inorganic polymeric new materials. J. Therm. Anal. 37, 1633–1656.

De Silva, P., Sagoe-Crenstil, K., Sirivivatnanon, V., 2007. Kinetics of geopolymerization: role of Al_2O_3 and SiO_2. Cem. Concr. Res. 37, 512–518.

Doebelin, N., Kleeberg, R., 2015. Profex: a graphical user interface for the Rietveld refinement program BGMN. J. Appl. Crystallogr. 48, 1573–1580.

Duminuco, P., Messiga, B., Riccardi, M.P., 1998. Firing process of natural clays. Some microtextures and related phase compositions. Thermochim. Acta 321, 185–190.

Duxson, P., Fernández-Jiménez, A., Provis, J.L., Lukey, G.C., Palomo, A., van Deventer, J.S.J., 2007. Geopolymer technology: the current state of the art. J. Mater. Sci. 42, 2917–2933.

Duxson, P., Lukey, G.C., van Deventer, J.S.J., 2007. Physical evolution of Na-geopolymer derived from metakaolin up to 1000 °C. J. Mater. Sci. 42, 3044–3054.

Essaidi, N., Samet, B., Baklouti, S., Rossignol, S., 2013. Effect of calcination temperature of Tunisian clay on the properties of geopolymers. Ceram–Silikáty 57, 251–257.

Essaidi, N., Samet, B., Baklouti, S., Rossignol, S., 2014. Feasibility of producing geopolymers from two different Tunisian clays before and after calcination at various temperatures. Appl. Clay Sci. 88-89, 221–227.

Fernandez, R., Martirena, F., Scrivener, K.L., 2011. The origin of the pozzolanic activity of calcined clay minerals: a comparison between kaolinite, illite and montmorillonite. Cem. Concr. Res. 41, 113–122.

Fernández-Jiménez, A., Puertas, F., 2001. Setting of alkali-activated slag cement. Influence of activator nature. Adv. Cem. Res. 13 (3), 115–121.

Fernández-Jiménez, A., Palomo, J.G., Puertas, F., 1999. Alkali-activated slag mortars mechanical strength behaviour. Cem. Concr. Res. 29, 1313–1321.

Ferone, C., Colangelo, F., Cioffi, R., Montagnaro, F., Santoro, L., 2013. Use of reservoir clay sediments as raw materials for geopolymer binders. Adv. Appl. Ceram. 112, 184–189.

Ferone, C., Liguori, B., Capasso, I., Colangelo, F., Cioffi, R., Cappelletto, E., Di Maggio, R., 2015. Thermally treated clay sediments as geopolymer source material. Appl. Clay Sci. 107, 195–204.

Franzini, M., Leoni, L., Saitta, M., 1972. A simple method to evaluate the matrix effects in X-ray fluorescence analysis. X-Ray Spectrom. 1, 151–154.

Franzini, M., Leoni, L., Saitta, M., 1975. Revisione di una metodologia analitica per fluorescenza-X, basata sulla correzione completa degli effetti di matrice. Rend. Soc. Ital. Mineral. Petrol. 31, 365–378.

Galván-Ruiz, M., Hernández, J., Baños, L., Noriega-Montes, J., Rodríguez-García, M.E., 2009. Characterization of calcium carbonate, calcium oxide, and calcium hydroxide as starting point to the improvement of lime for their use in construction. J. Mater. Civ. Eng. 21, 694–698.

García-Lodeiro, I., Fernández-Jiménez, A., Palomo, A., MacPhee, D.E., 2010. Effect of calcium additions on N-A-S-H cementitious gels. J. Am. Ceram. Soc. 93, 1934–1940.

García-Lodeiro, I., Palomo, A., Fernández-Jiménez, A., MacPhee, D.E., 2011. Compatibility studies between N-A-S-H and C-A-S-H gels. Study in the ternary diagram Na_2O-CaO-Al_2O_3-SiO_2-H_2O. Cem. Concr. Res. 41, 923–931.

García-Lodeiro, I., Maltseva, O., Palomo, A., Fernández-Jiménez, A., 2012. Hybrid alkaline cements. Part I: fundamentals. Rev. Rom. Mater. J. Mater 42, 330–335.

García-Lodeiro, I., Fernández-Jiménez, A., Palomo, A., 2013. Variation in hybrid cements over time. Alkaline activation of fly ash-portland cement blends. Cem. Concr. Res. 52, 112–122.

Gonzalez Garcia, F., Ruiz Abrio, M.T., Gonzalez Rodriguez, M., 1991. Effects of dry grinding on two kaolins of different degrees of crystallinity. Clay Miner. 26, 549–565.

Granizo, M.L., Blanco-Varela, A., Palomo, A., 2000. Influence of the starting kaolin on alkali-activated materials based on metakaolin. Study of the reaction parameters by isothermal conduction calorimetry. J. Mater. Sci. 35, 6309–6315.

Gualtieri, A.F., 2000. Accuracy of XRPD QPA using the combined Rietveld-RIR method. J. Appl. Crystallogr. 33, 267–278.

Gualtieri, A.F., Venturelli, P., 1999. In situ study of the goethite-hematite phase transformation by real time synchotron powder diffraction. Am. Mineral. 84, 895–904.

Guggenheim, S., Chang, Y.-H., Koster van Groos, A.F., 1987. Muscovite dehydroxylation: high-temperature studies. Am. Mineral. 72, 537–550.

Habert, G., Choupay, N., Escadeillas, G., Guillaume, D., Montel, J.M., 2009. Clay content of argillites: influence on cement based mortars. Appl. Clay Sci. 43, 322–330.

Hamzaoui, R., Muslim, F., Guessasma, S., Bennabi, A., Guillin, J., 2015. Structural and thermal behavior of proclay kaolinite using high energy ball milling process. Powder Technol. 271, 228–237.

He, C., Makovicky, E., Osbæck, B., 1994. Thermal stability and pozzolanic activity of calcined kaolin. Appl. Clay Sci. 9, 165–187.

He, C., Makovicky, E., Osbæck, B., 1995. Thermal stability and pozzolanic activity of calcined illite. Appl. Clay Sci. 9, 337–354.

He, C., Osbæck, B., Makovicky, E., 1995. Pozzolanic reactions of six principal clay minerals: activation, reactivity assessments and technological effects. Cem. Concr. Res. 25, 1691–1702.

Heller-Kallai, L., 2006. Thermally modified clay minerals. In: Bergaya, F., Theng, B.K.G., Lagaly, G. (Eds.), Handbook of Clay Science. Elsevier Ltd., pp. 289–308.

van Jaarsveld, J.G.S., van Deventer, J.S.J., Lukey, G.C., 2002. The effect of composition and temperature on the properties of fly ash- and kaolinite-based geopolymers. Chem. Eng. J. 89, 63–73.

Kamseu, E., Rizzuti, A., Leonelli, C., Perera, D., 2010. Enhanced thermal stability in K_2O-metakaolin-based geopolymer concretes by Al_2O_3 and SiO_2 fillers addition. J. Mater. Sci. 45, 1715–1724.

Kaps, C., Hohmann, M., 2010. Geopolymer binders in composite cements and ceramic-like materials. Adv. Sci. Technol. 69, 31–40.

Khater, H.M., 2012. Effect of calcium on geopolymerization of aluminosilicate wastes. J. Mater. Civ. Eng. 24, 92–101.

Lee, W.K.W., van Deventer, J.S.J., 2002. The effect of ionic contaminants on the early-age properties of alkali-activated fly ash-based cements. Cem. Concr. Res. 32, 577–584.

Letsch, J., Noll, W., 1983. Phase formation in several ceramic subsystems at 600 °C-1000 °C as a function of oxygen fugacity. Berichte der Dtsch. Keramischen Gesellschaft 7, 259–267.

Mackenzie, K.J.D., Welter, M., 2014. Geopolymer (aluminosilicate) composites: synthesis, properties and applications. In: Advances in Ceramic Matrix Composites. pp. 445–470.

MacKenzie, K.J.D., Brew, D.R.M., Fletcher, R.A., Vagana, R., 2007. Formation of aluminosilicate geopolymers from 1:1 layer-lattice minerals pre-treated by various methods: a comparative study. J. Mater. Sci. 42, 4667–4674.

Madejová, J., 2003. FTIR techniques in clay mineral studies. Vib. Spectrosc. 31, 1–10.

Maggetti, M., Neururer, C., Ramseyer, D., 2011. Temperature evolution inside a pot during experimental surface (bonfire) firing. Appl. Clay Sci. 53, 500–508.

Maritan, L., Nodari, L., Mazzoli, C., Milano, A., Russo, U., 2006. Influence of firing conditions on ceramic products: experimental study on clay rich in organic matter. Appl. Clay Sci. 31, 1–15.

Moore, D.M., Reynolds Jr, R.C., 1997. X-Ray Diffraction and the Identification and Analysis of Clay Minerals, Second edition Oxford University Press, New York.

Palomo, A., Blanco-Varela, M.T., Granizo, M.L., Puertas, F., Vazquez, T., Grutzeck, M.W., 1999. Chemical stability of cementitious materials based on metakaolin. Cem. Concr. Res. 29, 997–1004.

Palomo, A., Grutzeck, M.W., Blanco, M.T., 1999. Alkali-activated fly ashes: A cement for the future. Cem. Concr. Res. 29, 1323–1329.

Pesenti, H., Leoni, M., Scardi, P., 2008. XRD line profile analysis of calcite powders produced by high energy milling. Z. Krist. (Suppl. 27), 143–150.

Rathossi, C., Pontikes, Y., 2010. Effect of firing temperature and atmosphere on ceramics made of NW Peloponnese clay sediments. Part I: reaction paths, crystalline phases, microstructure and colour. J. Eur. Ceram. Soc. 30, 1841–1851.

Riccardi, M.P., Messiga, B., Duminuco, P., 1999. An approach to the dynamics of clay firing. Appl. Clay Sci. 15, 393–409.

Ruiz-Santaquiteria, C., Fernández-Jiménez, A., Skibsted, J., Palomo, A., 2013. Clay reactivity: production of alkali activated cements. Appl. Clay Sci. 73, 11–16.

Sánchez-Soto Wiewióra, A., Avilés, M.A., Justo, A., Pérez-Maqueda, L.A., Pérez-Rodríguez, J.L., Bylina, P., 1997. Talc from Puebla de Lillo, Spain. II. Effect of dry grinding on particle size and shape. Appl. Clay Sci. 12, 297–312.

Sánchez-Soto, P.J., Pérez-Rodriguez, J.L., 1989. Formation of mullite from pyrophyllite by mechanical and thermal treatments. J. Am. Ceram. Soc. 72, 154–157.

Sánchez-Soto, P.J., Justo, A., Pérez-Rodríguez, J.L., 1994. Grinding effect on kaolinite-pyrophyllite-illite natural mixtures and its influence on mullite formation. J. Mater. Sci. 29, 1276–1283.

Sánchez-Soto, P.J., de Haro, Jiménez, del C, M., Pérez-Maqueda, L.A., Varona, I., Pérez-Rodríguez, J.L., 2000. Effects of dry grinding on the structural changes of kaoli- nite powders. J. Am. Ceram. Soc. 83, 1649–1657.

Seiffarth, T., Hohmann, M., Posern, K., Kaps, C., 2013. Effect of thermal pre-treatment conditions of common clays on the performance of clay-based geopolymeric binders. Appl. Clay Sci. 73, 35–41.

Snellings, R., Mertens, G., Elsen, J., 2012. Supplementary cementitious materials. Rev. Mineral. Geochem. 74, 211–278.

Souri, A., Kazemi-Kamyab, H., Snellings, R., Naghizadeh, R., Golestani-Fard, F., Scrivener, K., 2015. Pozzolanic activity of mechanochemically and thermally activated kaolins in cement. Cem. Concr. Res. 77, 47–59.

Srasra, E., Bergaya, F., Fripiat, J.J., 1994. Infrared spectroscopy study of tetrahedral and octahedral substitutions in an interstratified illite-smectite clay. Clay Clay Miner. 42, 237–241.

Suraj, G., Iyer, C.S.P., Rugmini, S., Lalithambika, M., 1997. The effect of micronization on kaolinites and their sorption behaviour. Appl. Clay Sci. 12, 111–130.

Temuujin, J., van Riessen, A., Williams, R., 2009. Influence of calcium compounds on the mechanical properties of fly ash geopolymer pastes. J. Hazard. Mater. 167, 82–88.

Tickell, F.G., 1965. The Techniques of Sedimentary Mineralogy. Elsevier Pub. Co., Amsterdam.

Tironi, A., Trezza, M.A., Scian, A.N., Irassar, E.F., 2013. Assessment of pozzolanic activity of different calcined clays. Cem. Concr. Compos. 37, 319–327.

Trindade, M.J., Dias, M.I., Coroado, J., Rocha, F., 2009. Mineralogical transformations of calcareous rich clays with firing: a comparative study between calcite and dolomite rich clays from Algarve, Portugal. Appl. Clay Sci. 42, 345–355.

Tschegg, C., Ntaflos, T., Hein, I., 2009. Thermally triggered two-stage reaction of carbonates and clay during ceramic firing - a case study on bronze age Cypriot ceramics. Appl. Clay Sci. 43, 69–78.

Tyagi, B., Chudasama, C.D., Jasra, R.V., 2006. Determination of structural modification in acid activated montmorillonite clay by FT-IR spectroscopy. Spectrochim. Acta-Part A Mol. Biomol. Spectrosc. 64, 273–278.

Ufer, K., Kleeberg, R., Bergmann, J., Dohrmann, R., 2012. Rietveld refinement of disordered illite-smectite mixed layered structures by a recursive algorithm. I: one-dimensional patterns. Clay Clay Miner. 60, 507–534.

Ufer, K., Kleeberg, R., Bergmann, J., Dohrmann, R., 2012. Rietveld refinement of disordered illite/smectite mixed layered minerals with a recursive algorithm. II: powder pattern refinement and quantitative phase analysis. Clay Clay Miner. 60, 535–552.

Vaculíková, L., Plevová, E., 2005. Identification of clay minerals and micas in sedimentary rocks. Acta Geodyn. Geomater. 2, 167–175.

Vizcayno, C., de Gutiérrez, R.M., Castello, R., Rodriguez, E., Guerrero, C.E., 2010. Pozzolan obtained by mechanochemical and thermal treatments of kaolin. Appl. Clay Sci. 49, 405–413.

Xu, H., van Deventer, J.S.J., 2002. The geopolymerisation of alumino-silicate minerals. Int. J. Miner. Process. 59, 247–266.

Yip, C.K., Lukey, G.C., Van Deventer, J.S.J., 2005. The coexistence of geopolymeric gel and calcium silicate hydrate at the early stage of alkaline activation. Cem. Concr. Res. 35, 1688–1697.

Yip, C.K., Provis, J.L., Lukey, G.C., van Deventer, J.S.J., 2008. Carbonate mineral addition to metakaolin-based geopolymers. Cem. Concr. Compos. 30, 979–985.
Yu, P., Kirkpatrick, R.J., Poe, B., McMillan, P.F., Cong, X., 1999. Structure of calcium silicate hydrate (C-S-H): near-, mid-, and far-infrared spectroscopy. J. Am. Ceram. Soc. 82, 742–748.